Available online at www.sciencedirect.com
ScienceDirect
Ceramics International 36 (2010) 797–801
CERAMICS INTERNATIONAL
www.elsevier.com/locate/ceramint

Short communication

Interfacial and fouling effects on diffusional permeability across a composite ceramic membrane

L. Pelaez, M.I. Vázquez, J. Benavente *

Grupo de Caracterización Electrocinética en Membranas e Interfases, Departamento de Física Aplicada I. Facultad de Ciencias, Universidad de Málaga, E-29071 Málaga, Spain

Received 27 July 2009; received in revised form 30 July 2009; accepted 2 September 2009
Available online 12 October 2009

Abstract

Diffusional NaCl transport across a microporous ceramic membrane was studied by measurements carried out at a constant feed concentration (C_f = 0.01 equiv./l) but different solutions stirring rates ($0 \leq \nu$ (rpm) ≤ 1000), which allows the determination of both membrane system and true membrane diffusional permeability (P_{sm} and P_s, respectively). Differences between both values are related with the stagnant solution layer on the membrane surface, and its thickness was also determined from these measurements. Moreover, modification in diffusional permeability and polarization layer thickness as a result of membrane static protein fouling due to membrane–protein contact for two different protein solution concentrations (0.5 and 2 g/l of bovine serumalbumin) was also studied and correlated with the system structure.

Keywords: Ceramic membrane; Diffusional permeability; Concentration–polarization; Protein fouling

1. Introduction

Membrane technology is nowadays commonly used for separation of liquid mixtures in filtration, dialysis or fractioning of polymer mixtures processes. Concentration–polarization or the increase of solute concentration at the membrane/solution interface, which is directly related to the barrier effect of membranes, depends on both solution hydrodynamic conditions and solute/membrane–surface interactions [1,2]. High concentration–polarization might clearly reduce the efficiency of a separation process, mainly, in food and biotechnological applications. Another problem of great importance in these membrane separation applications is the ''membrane fouling'', which is usually associated to solute deposition on the membrane surface during filtration; this fact causes a significant decrease of the solution flow and, consequently, a reduction in the productivity of the process. Formation of a cake layer on the membrane surface (external fouling) and pore narrowing/plugging (internal fouling) are the most common fouling mechanisms [3,4]. Tangential solution flow in the membrane cell is commonly used in industrial applications to minimize those effects, but dead-end systems are more common at laboratory scale; moreover, membrane nature is also a critical point due to the needed of using chemical and temperature during cleaning protocols and, for that reason, ceramic membranes seem to be more adequate and durable than the common polymeric ones for such applications [5].

This work presents the characterization of mass transport across a composite ZrO_2/Al_2O_3 particles-layered membrane. Diffusive permeability was obtained from NaCl diffusion measurements performed at different solution stirring rates, which allow the determination of both ''membrane system'' and ''true'' membrane permeability as well as the thickness of the polarization layer. The reduction in membrane permeability after 48 h contact with protein solutions (bovine serumalbumin) allows the estimation of fouling effects as a function of both solution stirring rate and protein concentration.

2. Experimental

2.1. Membranes

A composite but symmetric ceramic membrane from Degussa (Germany) was studied. The Z100S membrane

* Corresponding author.
E-mail address: j_benavente@uma.es (J. Benavente).

0272-8842/$36.00
doi:10.1016/j.ceramint.2009.09.021

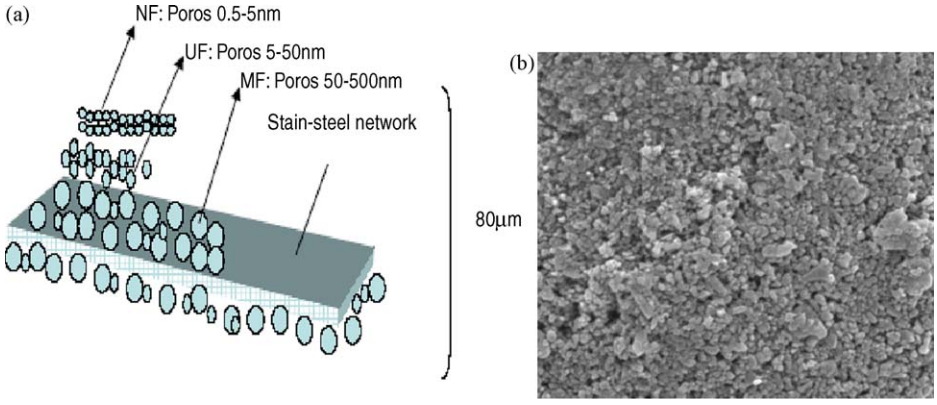

Fig. 1. (a) Membrane Z100S schematic representation, from Ref. [6]. (b) SEM micrograph of membrane Z100S surface.

consists of a fibrous stainless steel network covered by a sublayer of Al_2O_3 particles plus an external layer of ZrO_2 (see Fig. 1). The membrane geometrical parameters according to the supplier information [6] are: pore size of 0.1 μm, thickness of 80–100 μm and porosity of 25%.

Protein fouled samples were achieved by maintaining for 48 h one of the membrane surfaces in contact with a solution containing 0.5 or 2 g/l of bovine seroalbumin (or BSA, 66 kDa molecular weight from Sigma–Aldrich). The fouled samples will be named as Z100S/BSA-0.5 and Z100S/BSA-2, respectively.

2.2. Salt diffusion measurements

Measurements were performed in the dead-end test cell schematically shown in Fig. 2a. The membrane was clamped between two glass half-cells by using silicone rubber rings, and two magnetic stirrers were placed at the bottom of the half-cells to minimize the concentration–polarization at the membrane surfaces.

Salt diffusion measurements were performed with aqueous NaCl solutions at different concentrations, at room temperature (25 ± 2) °C, standard pH (5.8 ± 0.2). In these experiments the membranes separate a concentrated (feed) solution (C_f = 0.01 M) from a receiving diluted solution (C_v), which was initially distilled water. Time variation of feed and receiving solution concentrations was determined by measuring conductivity changes (σ_f and σ_r, respectively) by means of a conductivity cell placed in each semi-camera and connected each one to a digital conductivity meter (Crison GLP 31). In order to study the effect of concentration–polarization on salt diffusion, measurements were carried out at six different solutions stirring rates ν ranging between 0 and 1000 rpm.

3. Results and discussion

The solute transport across a membrane is represented by the diffusional permeability, P_s, which can be obtained from diffusion measurements at steady-state by using Fick's first low:

$$J_s = \frac{dn}{dt} = P_s \Delta C^m = P_s(C_f^m - C_r^m) \quad (1)$$

where J_s and ΔC^m are the solute flow and the concentration difference at both membrane sides, respectively. However, due to the solute barrier effect presented by the membrane, differences between bulk solution concentrations (C_i) and membrane surface concentrations (C_i^m) can exist as is schematically indicated in Fig. 2b.

If P_{sm} denotes the permeability for the membrane system, that is, the membrane plus the stagnant solution layers near the membrane surfaces, and $\Delta C = (C_f - C_r)$ is the difference between bulk feed and receiving solutions, Eq. (1) can also be expressed as:

$$J_s = P_{sm} \Delta C = P_{sm}(C_f - C_r) \quad (2)$$

Eq. (2) can also be expressed as:

$$\frac{dC_r}{C_f - C_r} = \frac{S_m}{V_o} P_{sm}\, dt \quad (3)$$

V_o and S_m are the volume of the receiving cell and the membrane area, respectively. Taking into account the mass continuity: $C_f^o + C_r^o = C_f^t + C_r^t = \text{cte}$, where C_f^o and C_r^o indicate the initial concentrations and C_f^t and C_r^t correspond to time t, the following expression is obtained [7]:

$$\ln\left[1 - \left(\frac{2C_r}{C_f}\right)\right] = -2\left[\frac{S_m}{V_o\ \Delta x_m}\right] P_{sm} t \quad (4)$$

where Δx_m represents the membrane thickness. Time evolution of solution concentration at different stirring rates, ν, is shown

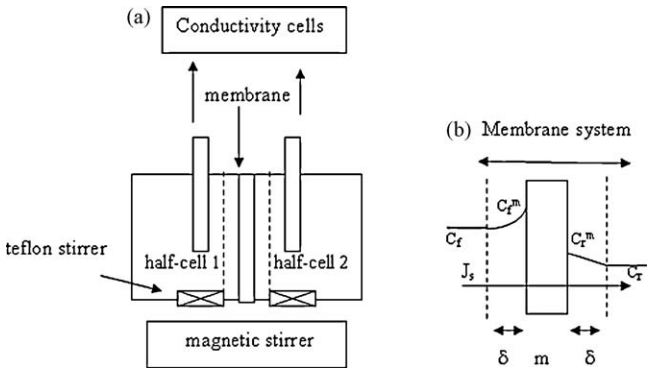

Fig. 2. (a) Measuring cell; (b) representation of membrane system: membrane plus polarization layers (no scale dimensions) and bulk solution concentrations.

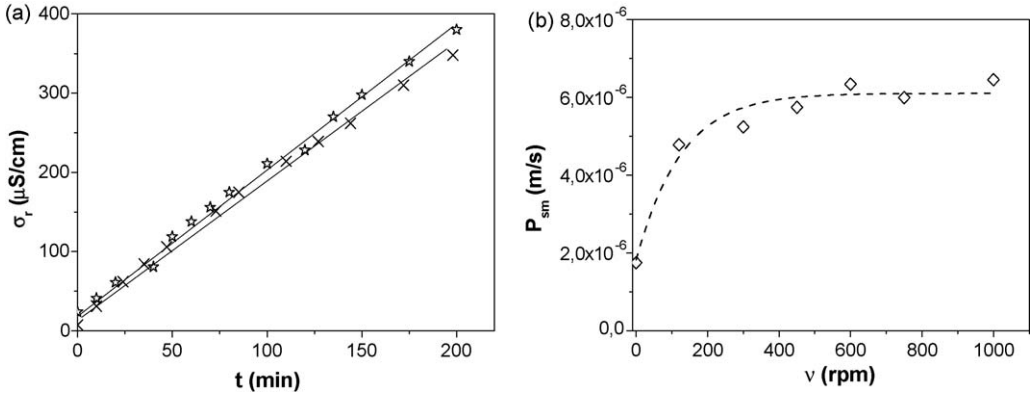

Fig. 3. (a) Receiving solution conductivity versus time for two stirring rates: 200 rpm (×) and 550 rpm (☆) Z100S. (b) Membrane system permeability as a function of solution stirring rate: (◇) experimental values; dotted line represents the fit according to Eq. (5).

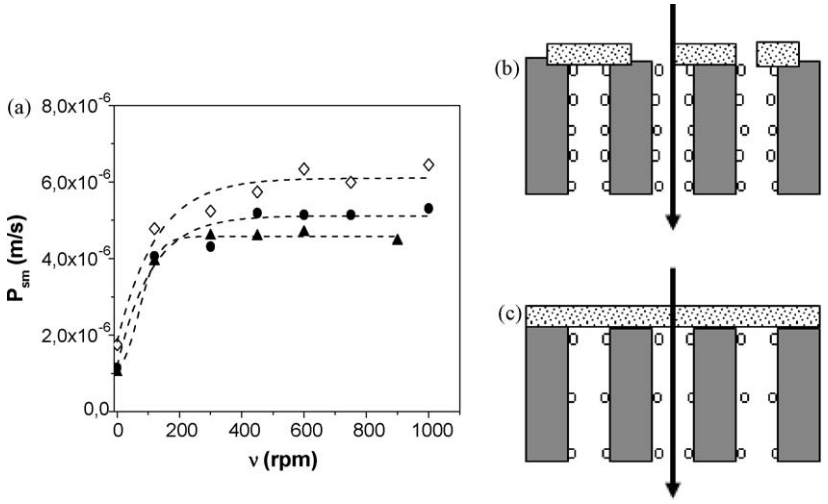

Fig. 4. (a) Comparison of P_{sm} values at different solution stirring rates for clean Z100S (◇), Z100S/BSA-0.5 (●) and Z100S/BSA-2 (▲) membranes. Schematic representation of two possible porous membrane fouling configurations: (b) partial membrane surface cover by cake layer and higher pore adsorption and (c) total cake layer covering membrane surface and lower pore adsorption.

in Fig. 3a; P_{sm} values were obtained by the slope of the straight lines (linear fit) according to Eq. (4).

Variation of P_{sm} with the stirring rate of the external solutions is shown in Fig. 3b, where the increase of the membrane system permeability with ν indicates the reduction of stagnant layers. ''True'' membrane permeability, P_s, can be obtained from the P_{sm} values obtained at different solutions celerities by using the following expression [8,9]:

$$P_{ms} = \frac{P_s(1+\alpha\nu)}{1+\alpha\nu+2[P_s/P_s^o]} \quad (5)$$

where α is an empirical parameter and $P_s^o = D_s^o/\delta$, being D_s^o the solute water diffusion coefficient and δ the thickness of the polarization layer. Eq. (5) allows the determination of both P_s and δ by the non-linear fitting of the values shown in Fig. 3b and the obtained results were: P_s (m/s) = 6.5×10^{-6} m/s and δ = 0.33 mm.

As can be observed in Fig. 3, a stirring rate of 500 rpm seems to be sufficient to minimized interfacial effects for Z100S membranes, although this point should be related with the morphology and it must be determined when comparison with different membranes are compared.

The adsorption/deposition of protein on the membrane surfaces as a result of fouling should modify both transport parameters and interfacial effects determined for the clean sample. For that reason, NaCl diffusion measurements across

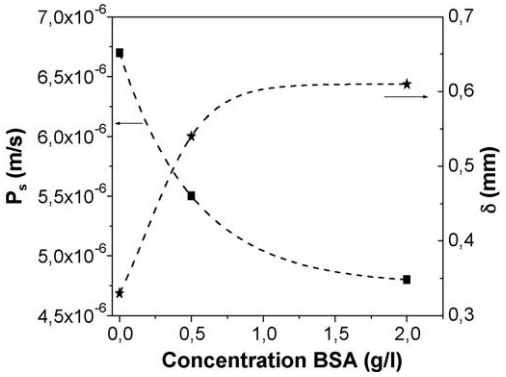

Fig. 5. Membrane permeability, P_s (■), and polarization layer thickness, δ (★), as a function of BSA concentration.

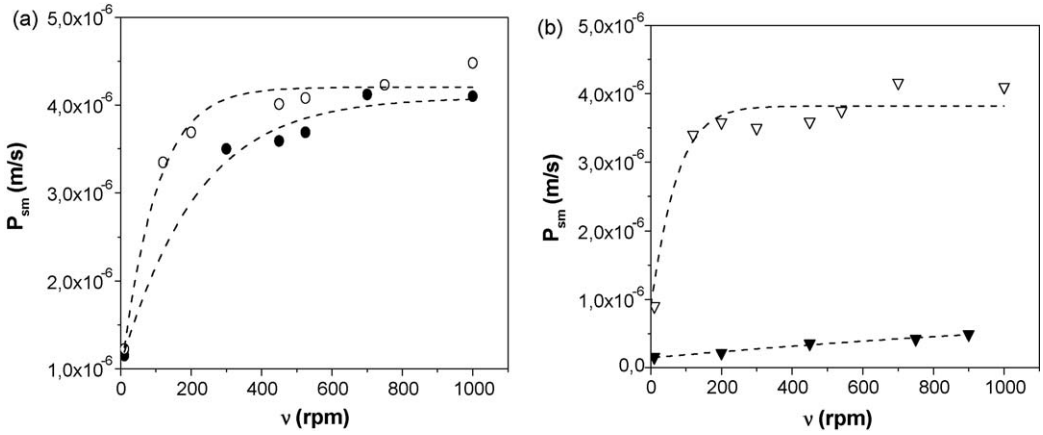

Fig. 6. Effect of BSA fouling on system permeability across two polymeric membranes. (a) RC (○), RC-fouled (●); (b) PVDF (▽), PVDF-fouled (▼).

membranes Z100S/BSA-0.5 and Z100S/BSA-2 were also performed and membrane system permeability was obtained following the same procedure that previously used for clean Z100S sample. Fig. 4a shows a comparison of P_{sm} values at different solution stirring rates for the three studied membranes, where the same type of dependence but lower permeability values as a result of higher BSA concentration can be observed. Fig. 4b and c shows two possible fouling configurations for an ideal porous membrane, partial or total cover of membrane surface by a cake layer, respectively, which might cause permeability differences: in the first case, permeability reduction should not be very important due to the possibility for solute to move through free path-way in the cake layer and the different membrane average pore radius and solute size (NaCl); however, the total cover of the membrane surface by cake layer indicated in Fig. 4c may present an extra resistance for solute diffusion. Non-ideal or complex membrane structures could favor the effect associated to protein-plugging.

The non-linear fit of the values drawn in Fig. 4a for both fouled samples allow the determination of P_s and δ values and their variation as a function of BSA concentration is shown in Fig. 5. As can be observed, values in Fig. 5 do not show a linear dependence with BSA concentration; in fact, the permeability reduction caused by protein fouling is around 18% for the sample fouled with 0.5 g/l of BSA and it increases until 28% when the protein concentration is 2 g/l, while the increase of polarization layer thickness is 65 and 85%, respectively. These results clearly show a more significant fouling effect at low protein concentration.

The importance of the membrane election for protein filtration applications can clearly be manifested by comparing fouling effects on diffusional permeability across two porous membranes with similar morphology (average pore radius of 0.2 μm and porosity around 40%) but different material (polyvinylidenedifluoride or PVDF and regenerated cellulose or RC) as is shown in Fig. 6. Although P_{sm} values for clean PVDF and RC membranes are comparable according to their morphological similarity, a significant reduction in permeability was obtained for PVDF-fouled membrane (around 90%) which seems to be caused by a fouling configuration similar to that shown in Fig. 4c, but the RC-fouled membrane exhibits much lower permeability reduction (around 18%), probably due to the hydrophilic character of cellulose [10].

Although the studied Z100S membrane has slightly lower values for average pore radius and porosity, the comparison of P_s values for the three clean samples does not show significant differences among them, but very different results were obtained for the fouled samples (see Figs. 4a and 6); this point remarks the interest of ceramic membranes for food and biotechnological applications, which could even increase if the chemical and thermal compatibility of membranes is considered due to their great importance for cleaning procedures [5,11].

4. Conclusions

Diffusional permeability across a flat composite ceramic membrane (ZrO_2/Al_2O_3) for liquid filtration was determined by diffusion measurements at different solution stirring rates, which also allows the determination of the interfacial effect (concentration–polarization). A solution stirring celerity of 500 rpm seems to be sufficient to minimize concentration–polarization at the membrane surface.

The effect of protein (BSA) fouling on permeate flow was also studied and the results clearly show a no-linear dependence on BSA concentration for both NaCl diffusional permeability and polarization layer thickness, being its effect more significant at low protein concentration.

Acknowledgements

We thank the partial financial support to CICYT (Project MAT/2007-65065, Spain) and Junta de Andalucía (Excellence Project FQM-1764).

References

[1] M. Mulder, Basic Principles of Membrane Technology, Kluwer Academic Publishers, Dordrecht, The Netherland, 1992.
[2] V. Gekas, G. Trägardh, B. Hallström, Ultrafiltration Membrane Performance fundamentals, KF-Sigma, Lund (Sweden), 1993.

[3] G. Belford, R.H. Davis, A.L. Sydney, The behaviour of suspensions and macromolecular solutions in cross flow microfiltration, J. Membr. Sci. 96 (1994) 1.
[4] A.D. Marshall, P.A. Munro, G. Trägardh, The effect of protein fouling in microfiltration and ultrafiltration on permeate flux, protein retention and selectivity: a literature review, Desalination 91 (1993) 65.
[5] P.R. Bhave, Inorganic Membranes Synthesis, Characteristic and Applications, Van Nostrand Reinhold, New York, 1991.
[6] S. Augustin, V. Hennige, G. Hörpel, C. Hying, Ceramic but flexible: new ceramic membrane foil for fuel cell and batteries, Desalination 146 (2002) 23.
[7] D.L. Gilbert, T. Okano, T. Miyata, S.W. Kim, Macromolecular diffusion through collagen membranes, Int. J. Pharm. 47 (1988) 79.
[8] M.V. Barragán, C. Ruíz-Bauzá, Membrane potential and electrolyte permeation in cation-exchange membranes, J. Membr. Sci. 154 (1999) 261.
[9] A. Cañas, M.I. Vázquez, J. Benavente, Effect of polarisation layers on salt permeability across membranes with different structures, Desalination 146 (2002) 163.
[10] L. Pelaez, S. Escalera, M.I. Vázquez, V. Romero, J. Benavente, A study of interfacial effects on diffusional permeability and cation transport across membranes from different materials and structures, in: III Conference on Colloids and Interfaces, Granada (Spain), 2009.
[11] A.J. Burgraff, L. Cot, Fundamental of Inorganic Membranes Science and Technology, Elsevier, 1996.